Electronic Supplementary Information

Correlation Between ^{13}C Chemical Shifts and the Halogen Bonding Environment in a Series of Solid *para*-Diiodotetrafluorobenzene Complexes

Jasmine Viger-Gravel, Sophie Leclerc, Ilia Korobkov, and David L. Bryce*

*Author to whom correspondence is to be addressed.

Department of Chemistry and Center for Catalysis Research and Innovation

University of Ottawa

10 Marie Curie Private

Ottawa, Ontario, Canada K1N 6N5

Tel.: +1 613 562 5800 ext. 2018; Fax: +1 613 562 5170

E-mail: dbryce@uottawa.ca

Additional information on X-ray structure refinement

Structures of **1**, **3**, **4**, and **5** contain molecules of *p*-DITFB located on the inversion center. During the refinement of the structure for compound **2**, unusually large thermal motion parameters for several atoms in the *n*-Bu chains of the phosphonium cation suggested the positional disorder. Disorder was modeled for the last two carbon atoms in the aliphatic chains and occupancy factors for both disorder models were refined to a 50/50 ratio for both disordered fragments. Similar disorder was discovered for the aliphatic chains of the cations in the structures of **3** and **4**. Similar models of the disorder for two tail carbon atoms of two *n*-Bu residues were refined with occupancy factors of 50/50 and 45/55 for compound **3**. The structure of compound **4** was refined with occupancy factors of 67/33 and 50/50 for disorder models similar to those described for **2** and **3**. The structures **3** and **4** contain disordered molecules of *p*-DITFB located on the inversion center. In both cases, disorder was modeled as a rotation of the aryl ring around the I - I axis. In the case of **4**, the rotational angle was found to be 48.67(3.02)◦ whereas for **3** this angle was found to be 25.20(2.66)◦, describing two disordered positions of the aryl rings. In order to improve the refinement results, obtain acceptable thermal motion parameters, and retain desirable molecular geometry, several sets of restraints were applied during the refinement of both structures. During the data collection for **4** it was discovered that crystal contained two non-merohedrally twinned domains. Twinning issues were resolved by integrating the data with two independent orientation matrices and performing the refinement using the HKLF 5 reflection intensities file. Refinement of the domain contributions yielded a twinning ratio of 48.3%.

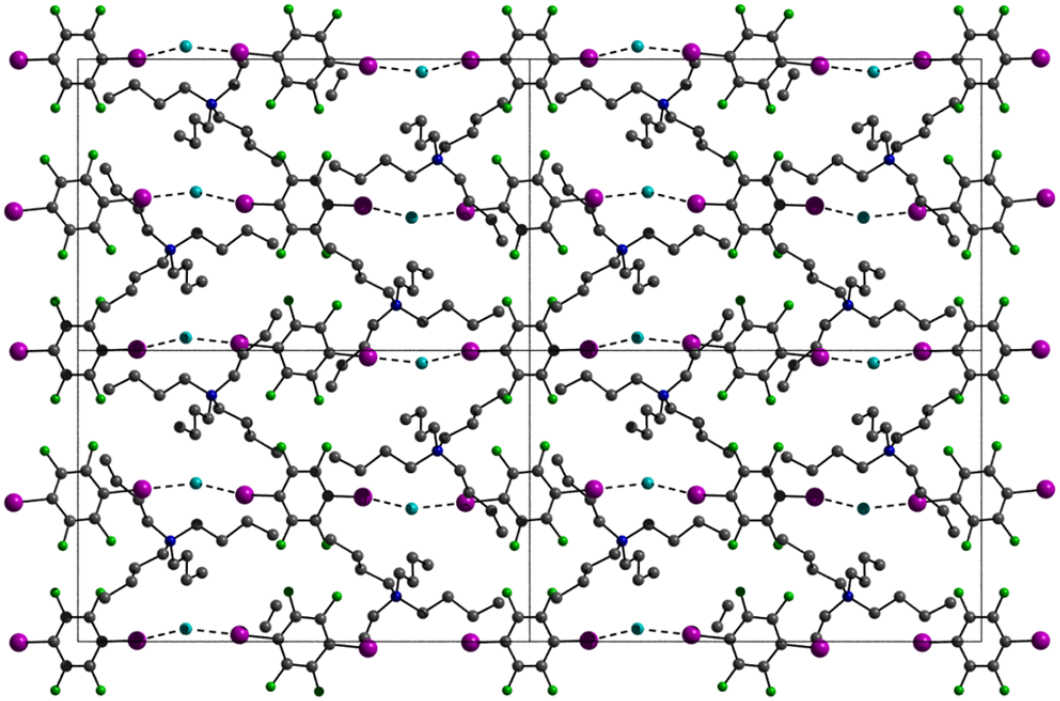

Figure S1. 2 x 2 x 2 cell of compound **1** along the *a* axis. The *p*-$C_6F_4I_2$ molecules form polymeric chains with a bridging chloride. Those chains alternate with rows of cations (*n*-Bu_4N^+) along the *a* axis. Hydrogens are omitted for clarity.

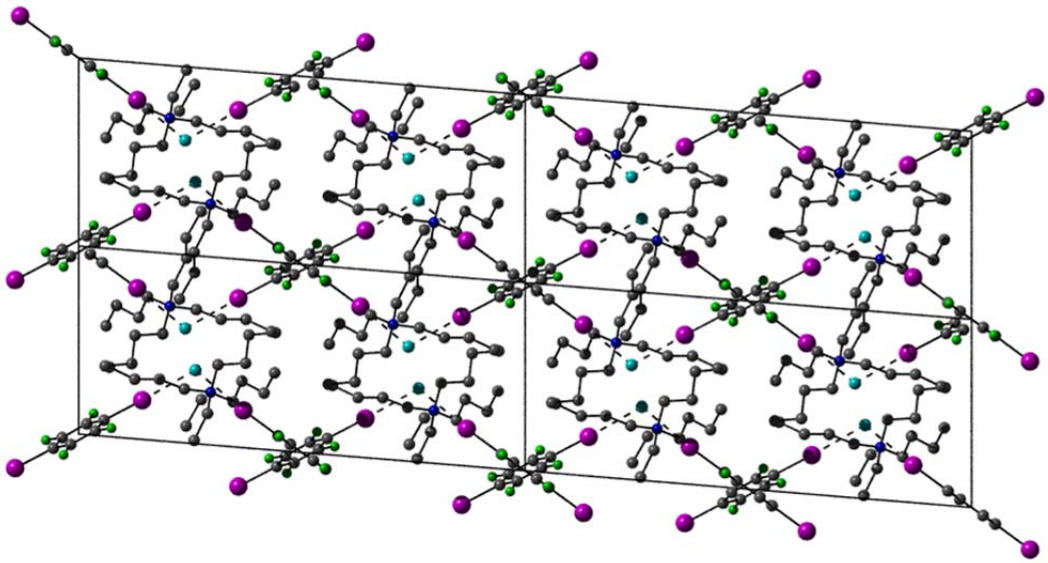

Figure S2. 2 x 2 x 2 cell of compound **1** along the *b* axis. Hydrogens are omitted for clarity.

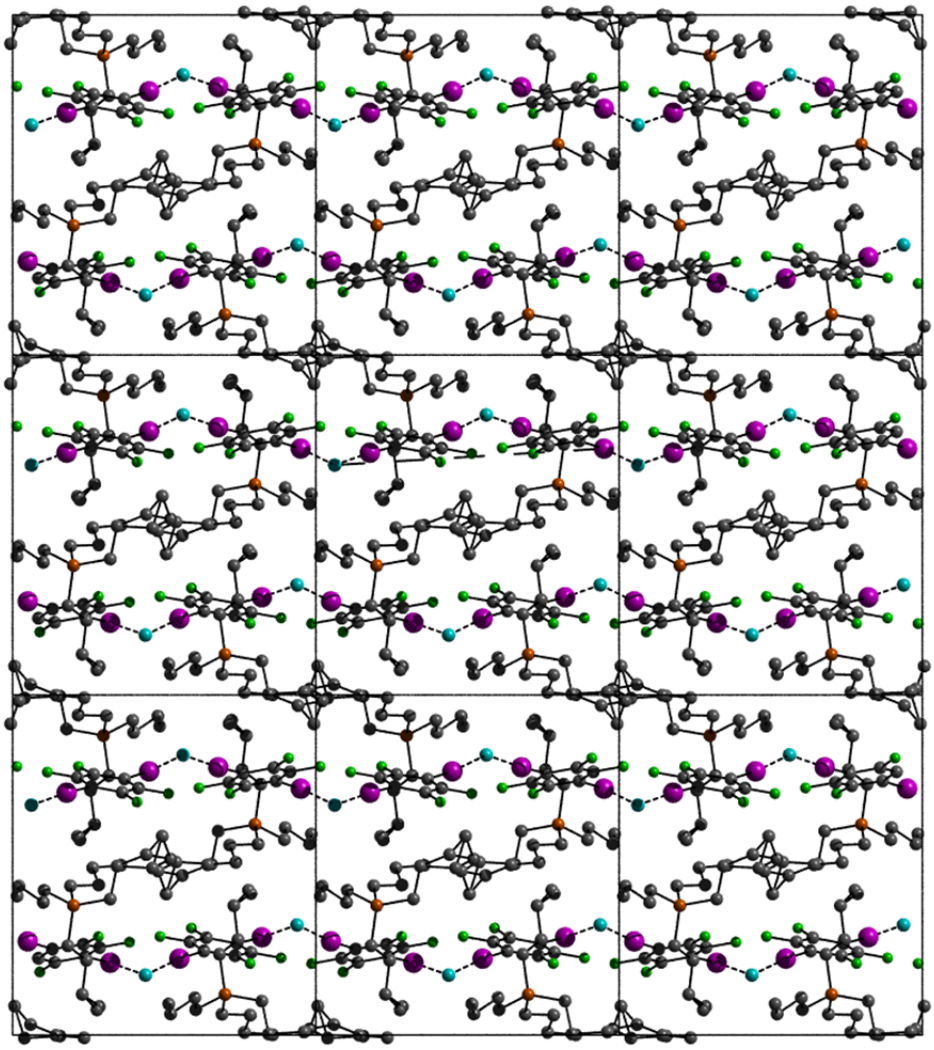

Figure S3. 3 x 3 x 3 cell of compound **2** shown along the *a* axis. The *p*-$C_6F_4I_2$ molecules form polymeric chains with a bridging chloride. Those chains alternate with rows of cations (*n*-Bu_4N^+) along the *a* axis. There is disorder at the end of the butyl chains. Hydrogens are omitted for clarity.

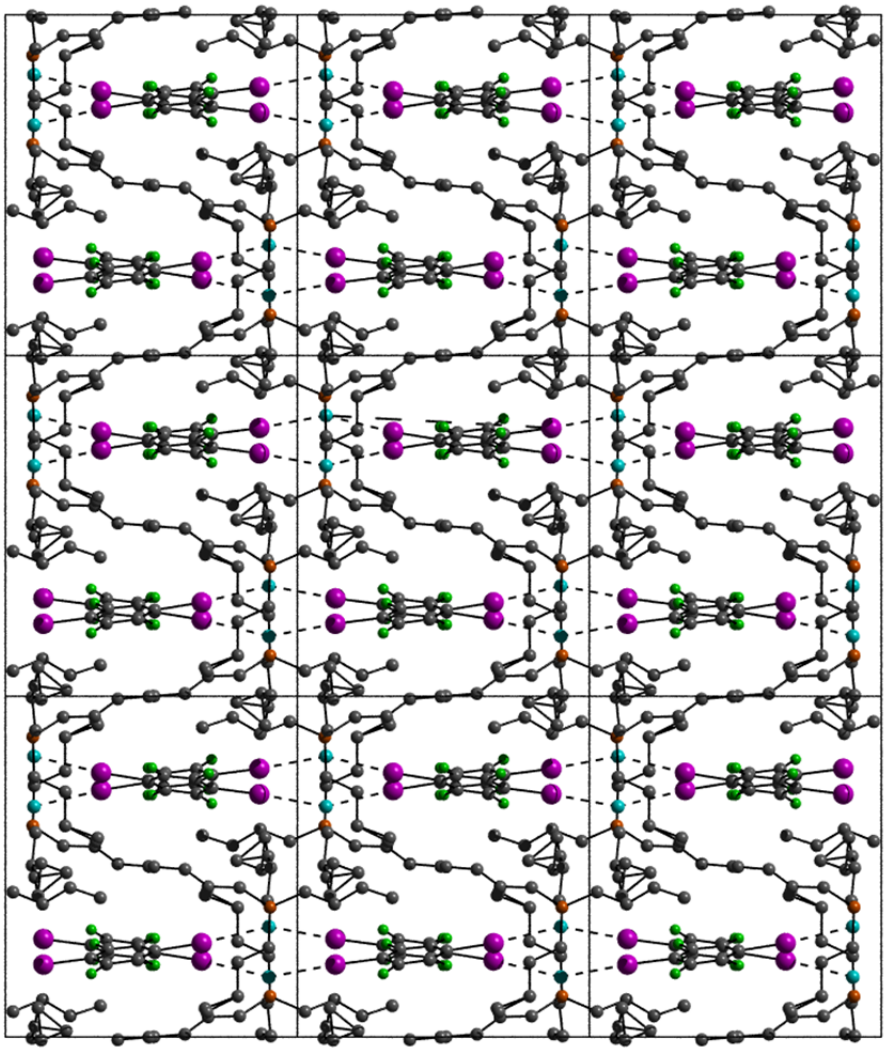

Figure S4. 3 x 3 x 3 cell of compound **2** shown along the *c* axis. Hydrogens are omitted for clarity.

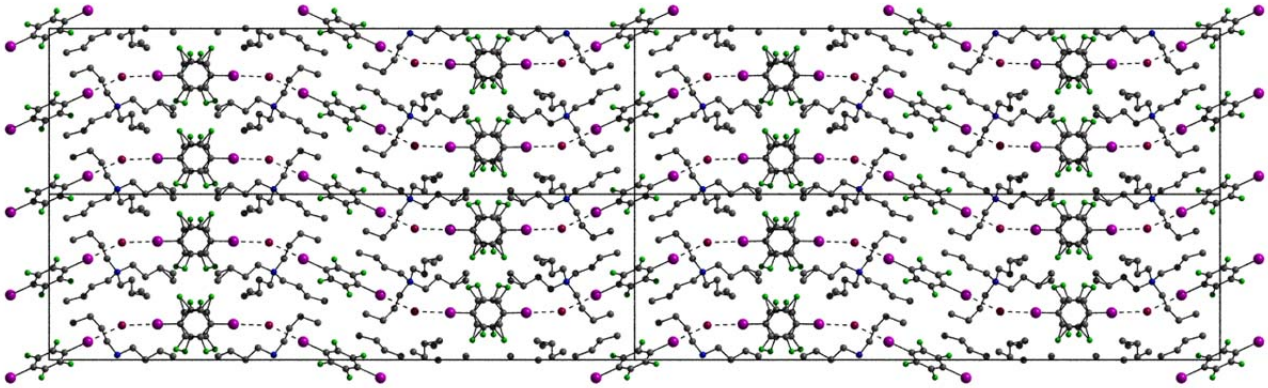

Figure S5. 2 x 2 x 2 cell of compound **3** shown along the *b* axis. The *p*-$C_6F_4I_2$ molecules form polymeric chains with a bridging bromide. Those chains alternate with rows of cations (*n*-Bu_4N^+) along the *b* axis. There is disorder at the end of the butyl chains. Hydrogens are omitted for clarity.

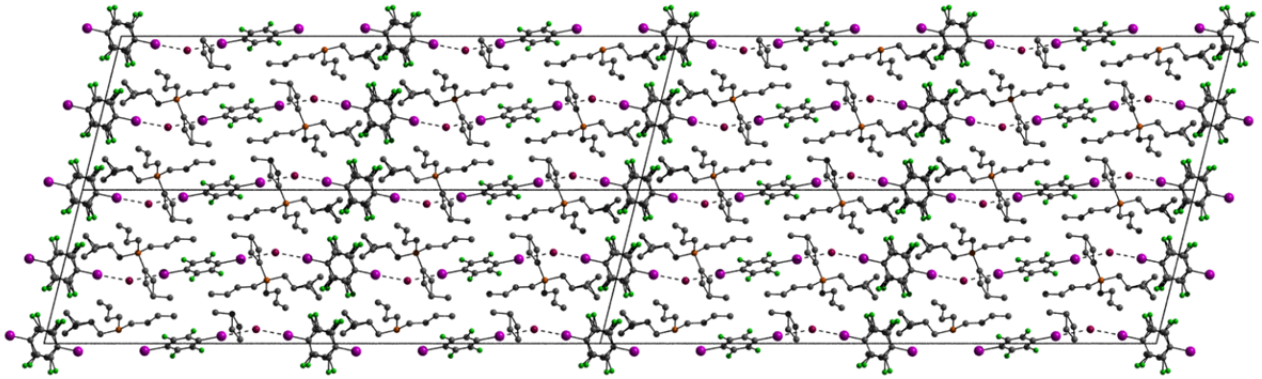

Figure S6. 2 x 2 x 2 cell of compound **4** shown along the *b* axis. The *p*-$C_6F_4I_2$ molecules form polymeric chains with a bridging bromide. Those chains alternate with rows of cations (*n*-Bu_4N^+) along the *b* axis. There is disorder at the end of the butyl chains. Hydrogens are omitted for clarity.

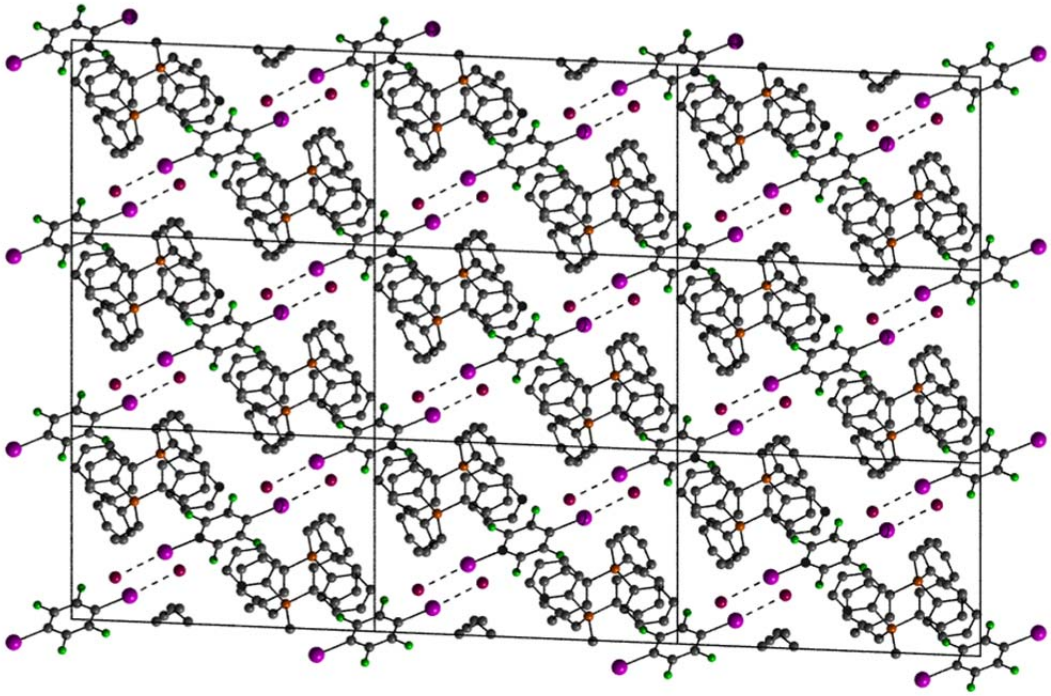

Figure S7. 3 x 3 x 3 cell of compound **5** shown along the *b* axis. The rows of $EtPh_3P^+$ cations alternate with rows of $[Br\cdots I—C_6F_4—I\cdots Br]^{2-}$ moieties. The ethyltriphenylphosphonium cations are associated two by two into the inversion centered phenyl embrace motif. Hydrogens are omitted for clarity.

Additional information on ^{13}C CPMAS SSNMR Spectra

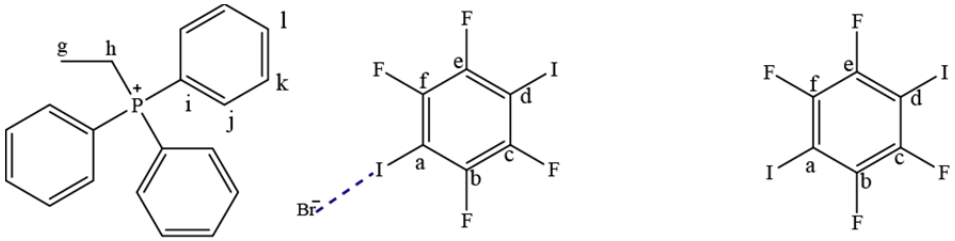

Figure S8. Labelling scheme for **5** and *p*-DITFB.

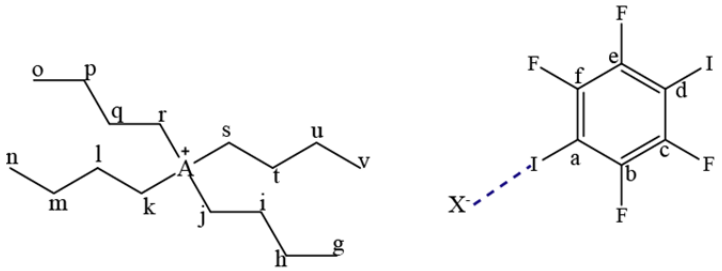

Figure S9. Labelling scheme for compounds **1** to **4**, where A is either P or N and X is Cl or Br.

Table S1. Experimental ^{13}C chemical shifts (ppm) of *p*-DITFB and compounds **1** to **5**

					C—I a,d	C—F b,c,e,f
p-DITFB					76.50	147.3
	CH_2 j ,k , r, s	CH_2 h,m,p,u	CH_2 i, l, q, t	CH_3 g, n, o, v		
1 [(*n*-Bu_4NCl)(*p*-DITFB)]	61.5-58.8	24.0-26.0	21.6-19.6	16.0, 14.4-13.0	83.92 80.64	148.0-145.5
2 [(*n*-Bu_4PCl)(*p*-DITFB)]	26.2-24.5	23.1-22.1	18.1-17.2	15.5-12.2	81.75 83.65	147.4-145.2
3 [(*n*-Bu_4NBr)(*p*-DITFB)]	62.5-60.0	26.2-24.6	22.9, 20.7-19.8	14.9, 14.6, 13.5, 12.2	84.72 81.84	147.2-145.7
4 [(*n*-Bu_4PBr)(*p*-DITFB)]	26.1-24.7	23.1-22.2	18.1-15.2	13.4-12.5	83.80 83.00	
	CH_3 g CH_2 h	i	j, k, l (CH)			
5 [($EtPh_3PBr)_2$(*p*-DITFB)]	7.9 17.2	112.7,116.5, 120.3-118.4	j, 131.3-129.3 k, 134.5-132.1 l, 138.5-135.9		84.50	147.2-145.0

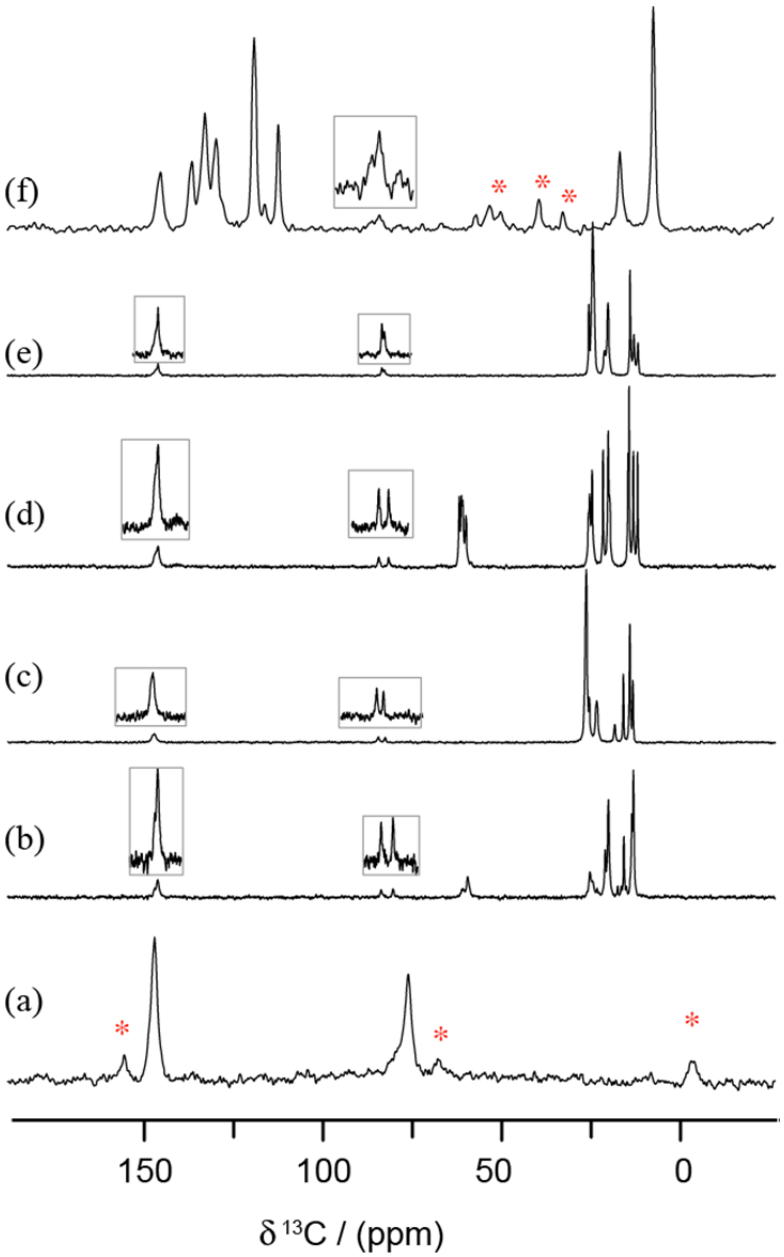

Figure S10. ^{13}C CPMAS SSNMR spectra acquired at 21.1 T of (a) *p*-DITFB, (b) [(*n*-Bu_4NCl)(*p*-DITFB)] (**1**), (c) [(*n*-Bu_4PCl)(*p*-DITFB)] (**2**), (d) [(*n*-Bu_4NBr)(*p*-DITFB)] (**3**), (e) [(*n*-Bu_4PBr)(*p*-DITFB)] (**4**), and (f) [$(EtPh_3PBr)_2$(*p*-DITFB)] (**5**). The insets show vertical expansions (4x). The asterisks denote spinning sidebands.

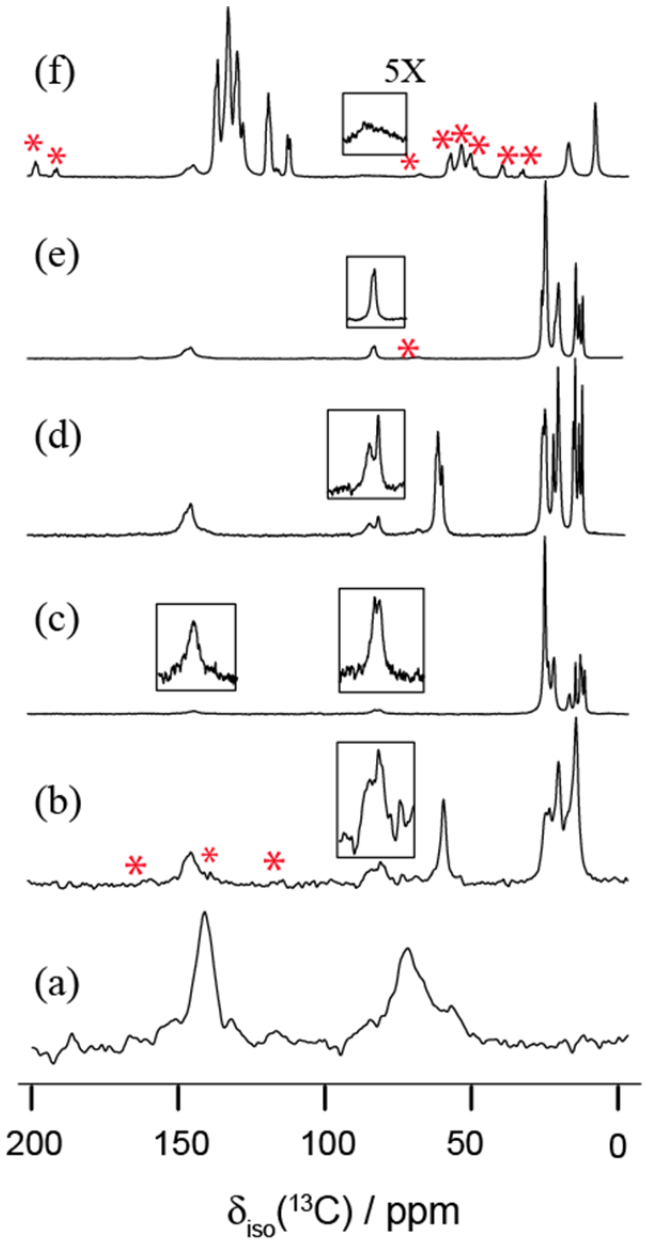

Figure S11. ^{13}C CPMAS SSNMR spectra acquired at 9.4 T of (a) *p*-DITFB, (b) [(*n*-Bu_4NCl)(*p*-DITFB)] (**1**), (c) [(*n*-Bu_4PCl)(*p*-DITFB)] (**2**), (d) [(*n*-Bu_4NBr)(*p*-DITFB)] (**3**), (e) [(*n*-Bu_4PBr)(*p*-DITFB)] (**4**), and (f) [$(EtPh_3PBr)_2$(*p*-DITFB)] (**5**). The insets show vertical expansions (4x, except for (f)). The asterisks denote spinning sidebands.

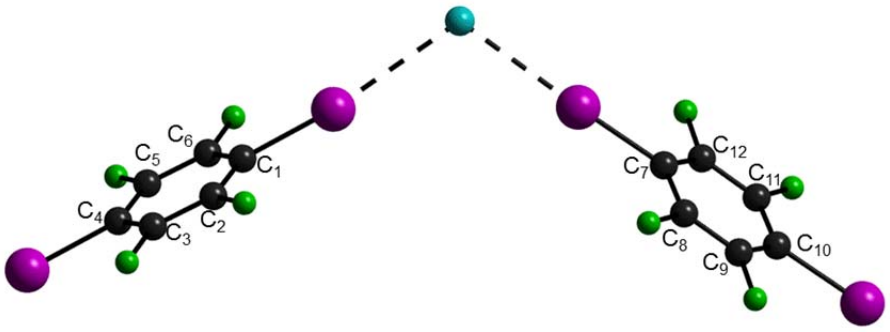

Figure S12. Labelling scheme for calculated $\delta_{iso}(^{13}C)$ values. (See Tables S2 to S10.)

Table S2. ZORA-DFT calculations of $\delta_{iso}(^{13}C)$ with scalar and spin orbit relativistic effects (GGA PBE, ZORA/TZP basis set)

	compound					
$\delta_{iso}(^{13}C)$	*p*-DITFB	**1**	**2**	**3**	**4**	**5**
$\underline{C_1}$—I---Cl[a]	74.03	87.52	97.62	103.32	122.74	98.10
$\underline{C_7}$—I---Cl		117.23	101.14	79.28	68.80	
$\underline{C_4}$—I	74.03	90.85	81.16	78.24	55.19	80.42
$\underline{C_{10}}$—I		67.76	79.17	76.40	103.97	
$\underline{C_2}$—F	147.38	151.68	152.44	152.19	151.78	153.07
$\underline{C_3}$—F	149.89	149.13	149.55	149.84	143.29	148.84
$\underline{C_5}$—F	147.39	149.02	149.83	149.76	149.81	149.18
$\underline{C_6}$—F	149.89	152.49	153.25	153.29	146.74	152.95
$\underline{C_8}$—F		152.73	152.12	137.26	151.47	
$\underline{C_9}$—F		149.64	149.94	134.03	148.84	
$\underline{C_{11}}$—F		150.30	149.89	142.12	148.06	
$\underline{C_{12}}$—F		152.01	153.13	145.61	151.90	

[a] Except for *p*-DITFB where this is simply $\underline{C_1}$-I.

Table S3. ZORA-DFT calculations of $\delta_{iso}(^{13}C)$ with scalar and spin orbit relativistic effects (GGA PBE, ZORA/TZP basis set, and AUG/ATZP for halide)

	Compound					
$\delta_{iso}(^{13}C)$	*p*-DITFB	**1**	**2**	**3**	**4**	**5**
$\underline{C_1}$—I---Cl[a]	74.03	86.79	96.85	95.10	121.30	97.57
$\underline{C_7}$—I---Cl		117.22	100.38	70.97	68.10	
$\underline{C_4}$—I	74.03	90.60	80.94	69.70	54.96	80.19
$\underline{C_{10}}$—I		67.48	78.92	67.62	103.70	
$\underline{C_2}$—F	147.38	151.64	151.89	151.60	151.40	152.77
$\underline{C_3}$—F	149.89	149.02	149.38	149.42	143.09	148.79
$\underline{C_5}$—F	147.39	148.90	149.77	149.41	149.44	149.10
$\underline{C_6}$—F	149.89	152.23	152.95	152.53	146.07	152.48
$\underline{C_8}$—F		152.32	151.55	136.71	151.09	
$\underline{C_9}$—F		149.49	149.76	133.65	148.72	
$\underline{C_{11}}$—F		150.14	149.81	141.75	148.04	
$\underline{C_{12}}$—F		151.66	152.87	145.10	151.73	

[a] Except for *p*-DITFB where this is simply $\underline{C_1}$-I.

Table S4. ZORA-DFT calculations of $\delta_{iso}(^{13}C)$ without relativistic effects (GGA PBE, TZP basis set)

	compound					
$\delta_{iso}(^{13}C)$	*p*-DITFB	**1**	**2**	**3**	**4**	**5**
$\underline{C_1}$—I---Cl[a]	91.94	127.10	126.57	127.94	126.75	128.14
$\underline{C_7}$—I---Cl		129.26	127.98	110.50	123.59	
$\underline{C_4}$—I	91.94	96.23	95.55	97.72	96.56	95.19
$\underline{C_{10}}$—I		96.26	94.41	90.34	95.01	
$\underline{C_2}$—F	148.34	153.45	154.50	154.18	153.97	154.75
$\underline{C_3}$—F	151.17	151.44	151.47	152.37	145.83	151.99
$\underline{C_5}$—F	148.34	151.66	152.42	152.36	151.95	152.20
$\underline{C_6}$—F	151.17	154.41	155.10	155.31	148.16	154.94
$\underline{C_8}$—F		154.87	154.04	140.04	153.44	
$\underline{C_9}$—F		151.49	152.00	136.52	151.68	
$\underline{C_{11}}$—F		152.31	152.30	144.95	151.05	
$\underline{C_{12}}$—F		154.12	155.02	148.00	154.13	

[a] Except for *p*-DITFB where this is simply $\underline{C_1}$-I.

Table S5. ZORA-DFT calculations of $\delta_{iso}(^{13}C)$ without relativistic effects (GGA PBE, TZP basis set, and AUG/ATZP for halide)

		compound				
$\delta_{iso}(^{13}C)$	*p*-DITFB	**1**	**2**	**3**	**4**	**5**
$\underline{C_1}$—I---Cl[a]	91.94	126.93	125.79	127.08	125.94	127.40
$\underline{C_7}$—I---Cl		129.12	127.24	109.79	122.63	
$\underline{C_4}$—I	91.94	95.98	95.35	97.51	96.30	94.81
$\underline{C_{10}}$—I		95.94	94.17	90.13	94.77	
$\underline{C_2}$—F	148.34	153.25	154.07	153.79	153.58	154.32
$\underline{C_3}$—F	151.17	151.33	151.34	152.24	145.68	151.87
$\underline{C_5}$—F	148.34	151.52	152.27	152.27	151.81	152.06
$\underline{C_6}$—F	151.17	154.02	154.60	154.78	147.63	154.45
$\underline{C_8}$—F		154.55	153.55	139.65	152.89	
$\underline{C_9}$—F		151.37	151.86	136.42	151.56	
$\underline{C_{11}}$—F		152.17	152.16	144.86	150.90	
$\underline{C_{12}}$—F		153.78	154.56	147.63	153.68	

[a] Except for *p*-DITFB where this is simply $\underline{C_1}$-I.

Table S6. ZORA-DFT calculations of $\delta_{iso}(^{13}C)$ with scalar and spin orbit relativistic effects (GGA revPBE, ZORA/TZP basis set)

		compound				
$\delta_{iso}(^{13}C)$	*p*-DITFB	**1**	**2**	**3**	**4**	**5**
$\underline{C_1}$—I---Cl[a]	72.12	85.87	95.53	93.80	119.27	96.13
$\underline{C_7}$—I---Cl		114.28	98.97	70.00	68.14	
$\underline{C_4}$—I	72.12	87.98	78.87	63.13	54.44	78.08
$\underline{C_{10}}$—I		66.30	76.93	65.63	100.21	
$\underline{C_2}$—F	144.57	148.62	149.42	149.00	148.97	150.05
$\underline{C_3}$—F	147.05	146.42	146.76	146.68	140.34	146.04
$\underline{C_5}$—F	144.57	146.30	146.96	146.65	146.72	146.42
$\underline{C_6}$—F	147.05	149.42	150.24	150.05	144.01	149.92
$\underline{C_8}$—F		149.84	149.12	134.38	148.25	
$\underline{C_9}$—F		146.65	147.13	131.32	146.31	
$\underline{C_{11}}$—F		147.27	147.01	139.14	145.52	
$\underline{C_{12}}$—F		149.15	150.14	142.55	148.72	

[a] Except for *p*-DITFB where this is simply $\underline{C_1}$-I.

Table S7. ZORA-DFT calculations of $\delta_{iso}(^{13}C)$ with scalar and spin orbit relativistic effects (GGA revPBE, ZORA/TZP basis set, and AUG/ATZP for halide)

	Compound					
$\delta_{iso}(^{13}C)$	*p*-DITFB	**1**	**2**	**3**	**4**	**5**
$\underline{C_1}$—I---Cl[a]	72.12	85.22	94.74	92.95	117.66	95.62
$\underline{C_7}$—I---Cl		114.17	98.21	69.53	67.54	
$\underline{C_4}$—I	72.12	87.73	78.64	67.91	54.19	77.84
$\underline{C_{10}}$—I		66.01	76.67	65.43	99.98	
$\underline{C_2}$—F	144.57	148.58	148.86	148.66	148.56	149.75
$\underline{C_3}$—F	147.05	146.31	146.59	146.55	140.13	145.98
$\underline{C_5}$—F	144.57	146.18	146.88	146.54	146.35	146.25
$\underline{C_6}$—F	147.05	149.16	149.95	149.55	143.29	149.43
$\underline{C_8}$—F		149.41	148.53	134.00	147.89	
$\underline{C_9}$—F		146.50	146.95	131.18	146.16	
$\underline{C_{11}}$—F		147.12	146.91	139.08	145.48	
$\underline{C_{12}}$—F		148.76	149.88	142.28	148.57	

[a] Except for *p*-DITFB where this is simply $\underline{C_1}$-I.

Table S8. ZORA-DFT calculations of $\delta_{iso}(^{13}C)$ without relativistic effects (GGA revPBE, TZP basis set)

	compound					
$\delta_{iso}(^{13}C)$	*p*-DITFB	**1**	**2**	**3**	**4**	**5**
$\underline{C_1}$—I---Cl[a]	89.68	124.41	123.89	125.27	124.12	125.55
$\underline{C_7}$—I---Cl		126.57	125.29	108.03	120.98	
$\underline{C_4}$—I	89.68	93.96	93.30	95.43	94.28	92.92
$\underline{C_{10}}$—I		93.99	92.15	88.17	92.76	
$\underline{C_2}$—F	145.55	150.54	151.57	151.25	151.03	151.81
$\underline{C_3}$—F	148.33	148.57	148.59	149.48	143.07	149.10
$\underline{C_5}$—F	145.55	148.77	149.52	149.45	149.04	149.30
$\underline{C_6}$—F	148.33	151.49	151.15	152.36	145.36	151.99
$\underline{C_8}$—F		151.93	151.11	137.39	150.51	
$\underline{C_9}$—F		148.61	149.11	133.93	148.79	
$\underline{C_{11}}$—F		149.41	149.40	142.22	148.17	
$\underline{C_{12}}$—F		151.20	152.08	145.21	151.12	

[a] Except for *p*-DITFB where this is simply $\underline{C_1}$-I.

Table S9. ZORA-DFT calculations of $\delta_{iso}(^{13}C)$ without relativistic effects (GGA revPBE, TZP basis set, and AUG/ATZP for halide)

		compound				
$\delta_{iso}(^{13}C)$	*p*-DITFB	**1**	**2**	**3**	**4**	**5**
$\underline{C_1}$—I---Cl[a]	89.68	124.20	123.09	124.39	123.28	124.76
$\underline{C_7}$—I---Cl		126.38	124.53	107.31	120.00	
$\underline{C_4}$—I	89.68	93.71	93.09	95.21	94.02	92.53
$\underline{C_{10}}$—I		93.67	91.91	87.95	92.52	
$\underline{C_2}$—F	145.55	150.33	151.12	150.85	150.62	151.36
$\underline{C_3}$—F	148.33	148.46	148.45	149.35	142.91	148.98
$\underline{C_5}$—F	145.55	148.63	149.37	149.36	148.90	149.17
$\underline{C_6}$—F	148.33	151.07	151.64	151.82	144.82	151.49
$\underline{C_8}$—F		151.60	150.61	136.99	149.95	
$\underline{C_9}$—F		148.49	148.96	133.83	148.67	
$\underline{C_{11}}$—F		149.26	149.26	142.12	148.02	
$\underline{C_{12}}$—F		150.83	151.61	144.82	150.67	

[a] Except for *p*-DITFB where this is simply $\underline{C_1}$-I.

Table S10. Summary of ZORA-DFT calculations of $\delta_{iso}(^{13}C)$ with relativistic effects of carbons covalently bonded to iodine

compound	experimental	PBE	PBE[a]	revPBE	revPBE[a]
p-DITFB	76.50(0.50)	74.03	74.03	72.12	72.12
1	83.92(0.01)	117.23	117.22	114.28	114.17
	80.64(0.02)	87.52	86.79	85.87	85.22
2	81.75(0.45)	97.62	96.85	95.53	94.74
	83.65(0.15)	101.14	100.38	98.97	98.21
3	84.72(0.10)	103.32	95.10	93.80	92.95
	81.84(0.01)	79.28	70.97	70.00	69.53
4	83.80(0.06)	122.74	121.3	119.27	117.66
	83.00(0.02)	68.80	68.10	68.14	67.54
5	84.50(0.25)	98.10	97.57	96.13	95.62

[a] Along with the usual basis used (ZORA/TZP), a diffuse basis set is added to the halide, AUG/ATZP.

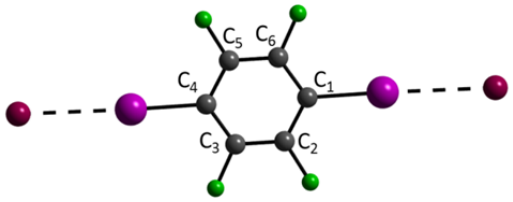

Figure S13. Labelling scheme for calculated $\delta_{iso}(^{13}C)$ values of GIPAW DFT calculations. (See Table S11.)

Table S11. GIPAW DFT calculations of $\delta_{iso}(^{13}C)$, with GGA PBE functional.[a]

$\delta_{iso}(^{13}C)$	*p*-DITFB[b]	**1**	**2**	**5**
$\underline{C_1}$—I---Cl	113.3	130.8	133.3	131.0
$\underline{C_4}$—I---Cl	113.3	132.8	137.1	131.0
$\underline{C_2}$—F	157.5	163.8	120.1	162.3
$\underline{C_3}$—F	162.6	163.0	101.6	162.9
$\underline{C_5}$—F	157.5	163.8	164.2	162.3
$\underline{C_6}$—F	162.6	163.0	167.0	162.9

[a] The kinetic energy cut-off is 450 eV and the k-point grid used is 1 x 1 x 1.

[b] The kinetic energy cut-off energy is 500 eV and the k-point grid is 2 x 2 x 1.

CASTEP software was used: Clark, S. J.; Segall, M. D.; Pickard, C. J.; Hasnip, P. J.; Probert, M. I. J.; Refson, K.; Payne,M. C. *Z. Kristallogr.* **2005**, 220, 567– 570; Pickard, C. J.; Mauri, F. *Phys. Rev. B* **2001**, 63, 245101.

Pseudopotentials used:

C 2|1.4|9.187|11.025|12.862|20UU:21UU(qc=6)[]
F 2|1.4|16.537|18.375|20.212|20UU:21UU(qc=7.5)[]
I 2|2|2|1.6|6|7.3|9.9|50U=-0.65U=+0:51U=-0.265U=+0[]
Cl 2|1.7|5.88|7.35|9.187|30UU:31UU:32LGG[]
P 2|1.8|3.675|5.512|6.982|30UU:31UU:32LGG[]
Br 2|2|2|1.4|5.6|6.6|8.8|40U=-0.74U=+0.25:41U=-0.295U=+0.25[]
H 1|0.8|3.675|7.35|11.025|10UU(qc=6.4)[]
N 2|1.5|11.025|12.862|14.7|20UU:21UU(qc=6)[]